Bolus Delay and Dispersion in Predictor Models in Acute Stroke

L. Willats[1], A. Connelly[1,2], S. Christensen[3,4], G. Donnan[2,5], S. Davis[4,6], and F. Calamante[1,2]

[1]Brain Research Institute, Florey Neuroscience Institutes, Melbourne, Australia, [2]Department of Medicine, University of Melbourne, Australia, [3]Department of Radiology, University of Melbourne, Australia, [4]Royal Melbourne Hospital, Melbourne, Australia, [5]Florey Neuroscience Institutes, Melbourne, Australia, [6]Department of Neurology, University of Melbourne, Australia

Introduction: In stroke, voxel-wise methods that combine acute imaging parameters with follow-up (F/U) imaging outcome in models to predict tissue outcome (e.g. [1]) have attracted considerable interest. Critical to the performance of these models is the choice and combination of acute parameters. Lorenz et al [2] have shown Local-AIF (LAIF) perfusion to be more predictive than Global AIF (GAIF) perfusion, which can be underestimated by bolus delay and dispersion (D/D) of the concentration time course (CTC) using standard SVD [3]. However, the decoupled effects of D/D have yet to be investigated in a predictor model. Indeed, recent studies have suggested that in addition to perfusion and diffusion deficits, D/D may also increase the risk of infarction [4,5]. In this work we develop predictor models using perfusion parameters decoupled from delay (GAIF and oSVD deconvolution [6]), and decoupled from both delay and dispersion (LAIFs and oSVD). To isolate the additional risk associated with delay and dispersion, further models including an estimate of D/D were also investigated.

Methods: Stroke patients without reperfusion were selected from the EPITHET trial [7], (<50% reduction in volume of Tmax abnormality subacutely, (Tmax=time-to-peak of the GAIF oSVD residue function, R)). 14 patients without severe motion artefact met this criterion. All had acute (3-6hrs) PWI and DWI, and F/U (3month) T2WI data. GAIF perfusion parameter maps (CBV, CBF_G, MTT_G, Tmax) [8], and LAIF perfusion parameter maps (CBF_L, MTT_L) [9] were calculated. Since the parameter Tmax is dependent on MTT as well as D/D [5], we also created adjusted first-moment parameter maps (FM_{adj} =FM[CTC]-FM[R]+Tmax), which reflect D/D but not MTT [9]. The acute DWI and F/U T2 images were coregistered to the acute PWI data [10], and all 8 acute parameter maps were normalised to contralateral WM values (by division (DWI,CBV,CBF), or difference (MTT, Tmax, FM_{adj})). Training regions were defined as in [1], excluding areas of CSF to avoid bias caused by brain shrinkage.

Eight different (logistic regression) GLM models [1] were trained using equal number of infracting and non infracting voxels (models A-H in Table 1). For each GLM coefficient b_k (associated with the acute parameter x_k), the bootstrap estimate of the mean was used [1]. For each patient (and each GLM), infarct probability maps for the ipsilateral hemisphere (*P*-maps) were generated using a jackknife model trained on the remaining 13 patients [1]. For each GLM, Receiver Operating Characteristic (ROC) curves were generated for the individual patient *P*-maps, as well as the aggregate ROC for all patient *P*-maps pooled together. For each ROC curve, the optimal operating point (OOP) was calculated (the probability threshold that gives the smallest false positive rate (FPR) for the largest true positive rate (TPR)), as well as the area under ROC curve, AUC (the probability that the model will predict higher probabilities in areas that do infarct compared with ones that do not).

For each GLM, the b_k coefficients and the associated Odds Ratio (OR) were also calculated from models trained with all the patient data. OR= $\exp(b_K)$ is the relative amount by which the predicted odds of infarction [odds=$P/(1-P)$, where P is the probability of infarction], increase (OR>1) or decrease (OR<1), per unit increase in the associated (normalised) parameter, whilst holding all other parameters constant.

All calculations were performed using Matlab.

Results: Table1: The AUC is higher for the models including a D/D parameter (Tmax or FM_{adj}), and also higher when the D/D parameter is combined in the GAIF models (F,G,H). Similarly, the sensitivity (TPR) and specificity (1-FPR) improve with the inclusion of a D/D parameter and are higher for the GAIF models. TPR and (1-FPR) are shown at the OOP of the pooled ROC curve, but show the same trend at the previously used [11] probability threshold of 0.5 (data not shown). The interquartile range (IQR) of the OOPs for the individual patient ROC curves is narrower for LAIF models including a D/D parameter than for GAIF models.

Figure 1 shows single slice *P*-maps for two patients for models A-H. For the patient in Figure 1a, only the LAIF models improve with the inclusion of Tmax and/or FM_{adj} (B,C,D better than A, but E,F,G,H approximately equal). For the patient in Figure 1b, the inclusion of Tmax and/or FM_{adj} improves both LAIF and GAIF GLM predictions (B,C,D better than A, and F,G,H better than E)

Figure 2 shows the Odds Ratios (OR) for each of the acute parameters within each GLM. A unit rise in DWI most strongly increases the odds across all models; a unit rise in CBF reduces the odds more for the LAIF models (A-D); a unit rise in Tmax has a much smaller influence when combined with FM_{adj} (D,H); a unit rise in FM_{adj} has similar influence across all relevant models (C,D,G,H).

Discussion: The *P*-maps in Figure 1a suggest that in this patient the inclusion of Tmax/FM_{adj} in the GLMs primarily adds information about dispersion: Given that the GAIF perfusion (CBF_G/MTT_G) is already coupled with dispersion, but dispersion bias is minimised in LAIF perfusion (CBF_L/MTT_L), the inclusion of a dispersion parameter improves the prediction of the LAIF models, but not the prediction of the GAIF. Conversely, the *P*-maps in Figure 1b, suggest that in this patient the inclusion of Tmax/FM_{adj} in the GLMs primarily adds information about delay: Delay information is lost in the both the GAIF and LAIF delay insensitive perfusion parameters, therefore the inclusion of a delay parameter improves both the prediction of the LAIF and GAIF models similarly. These two examples indicate that both delay and dispersion affect the infarction risk.

The GLM coefficients indicate that changes in CBF_L more strongly influence the odds of infarction than changes in CBF_G (Figure 2). A rise in CBF_G comprises of a rise in true CBF and/or a decrease in dispersion. Thus the OR for CBF_G is also weighted by the OR for dispersion. Similarly, due to its MTT dependence, a rise in Tmax comprises of a rise in D/D and/or a rise in MTT. When Tmax is combined in a GLM with FM_{adj} (D,H), its OR is close to 1, indicating that it does not add any further predictive information in these models. The AUCs are also larger for the GLMs containing FM_{adj} rather than Tmax, suggesting the FM_{adj} provides stronger predictive information than Tmax.

Based on the pooled ROC analysis, the AUCs (Table 1) indicate that the best predictions are obtained using GAIF perfusion, which although decoupled from delay, is still affected by dispersion. This may indicate that the LAIFs remove some important dispersion information that has not been added back into the GLM via FM_{adj} or Tmax. Including an estimate of the vascular transport function (VTF), (by for example deconvolving AIFs from the two hemispheres) may further assist in decoupling the infarct risk associated with dispersion, as well as generating more accurate predictions. Another possible explanation for the superiority of the GAIF models is the homogeneity of the perfusion maps. It may therefore be beneficial to smooth the acute parameters prior to training the GLM model.

Although the AUC values indicate that the GAIF models perform better overall, the AUC summarises model performance over all possible infarct probability thresholds. In practice a single probability threshold is used (e.g. the OOP). We found that that the IQR for the individual OOPs was smaller for the LAIF models (Table 1) suggesting that they will perform closer to optimum for a larger proportion of patients.

References: [1] Wu (2001) Stroke 32:933, [2] Lorenz (2006) JMRI 52:789, [3] Calamante (2000) MRM 44:466, [4] Christensen (2009) Stroke 40:2055, [5] Calamante (2010) Stroke 41:1169, [6] Wu (2003) MRM 50:164, [7] Butcher (2005) Stroke 36:1153, [8] www.cfin.au.dk/software/penguin [9] Willats (2010) ISMRM p1789, [10] Collins (1994) JCAT18:192. [11] Wu (2007) JCBFM 27:196.

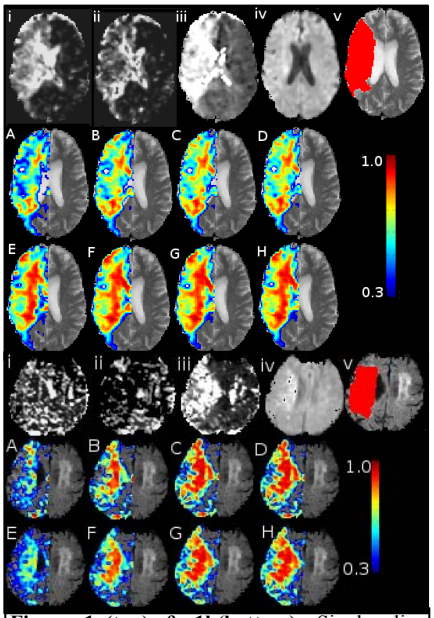

Figure 1a(top) & 1b(bottom): Single slice from 2 patients. Acute images MTT_G (i), MTT_L (ii), FM_{adj} (iii), DWI (iv), and F/U lesion (v). *P*-maps thresholded at 30% for models A-H.

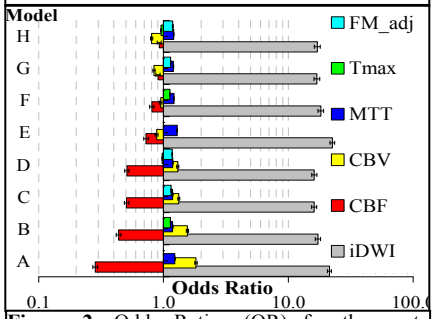

Figure 2: Odds Ratios (OR) for the acute parameters forming the GLM models A-H. OR=1 indicates no effect.

GLM		A	B	C	D	E	F	G	H
Acute parameters		DWI CBV CBF_L MTT_L	DWI CBV CBF_L MTT_L Tmax	DWI CBV CBF_L MTT_L FM_{adj}	DWI CBV CBF_L MTT_L Tmax FM_{adj}	DWI CBV CBF_G MTT_G	DWI CBV CBF_G MTT_G Tmax	DWI CBV CBF_G MTT_G FM_{adj}	DWI CBV CBF_G MTT_G Tmax FM_{adj}
Pooled	**AUC**	**0.748**	**0.801**	**0.824**	**0.824**	**0.805**	**0.835**	**0.848**	**0.847**
	OOP	44%	41%	40%	40%	43%	41%	41%	41%
	TPR	0.659	0.727	0.755	0.754	0.725	0.764	0.773	0.772
	1-FPR	0.717	0.751	0.768	0.769	0.752	0.775	0.796	0.798
Jack-knife	**OOP**	45%	43%	44%	43%	47%	41%	44%	41%
	IQR	**18%**	**13%**	**12%**	**11%**	**18%**	**17%**	**15%**	**15%**

Table 1: GLM models (A-H) and their acute parameters (top 2 rows). Models A-D use LAIF perfusion CBF_L and MTT_L, E-H use GAIF perfusion CBF_G and MTT_G. AUC, OOP, TPR and (1-FPR) (shown at the OOP) for the pooled ROC (middle 4 rows). Median and IQR of the OOP for the individual predictions (bottom 2 rows).